Understanding the effects of climate warming on streamflow and active groundwater storage in an alpine catchment, upper Lhasa River

Lu Lin[a,b], Man Gao[c], Jintao Liu[a,b*], Jiarong Wang[a,b], Shuhong Wang[a,b*], Xi Chen[a,b,c], Hu Liu[d]

[a] *State Key Laboratory of Hydrology-Water Resources and Hydraulic Engineering, Hohai University, Nanjing 210098, People's Republic of China*

[b] *College of Hydrology and Water Resources, Hohai University, Nanjing 210098, People's Republic of China*

[c] *Institute of Surface-Earth System Science, Tianjin University, Tianjin 300072, People's Republic of China*

[d] *Linze Inland River Basin Research Station, Chinese Ecosystem Research Network, Lanzhou 730000, People's Republic of China*

* *Corresponding author. Tel.: +86-025-83787803; Fax: +86-025-83786606.*

E-mail address: jtliu@hhu.edu.cn (J.T. Liu).

Abstract

Climate warming is changing streamflow regimes and groundwater storage in cold alpine regions. In this study, a headwater catchment named Yangbajain in the Lhasa River Basin is adopted as the study area for assessing streamflow changes and active groundwater storage in response to climate warming. The results show that both annual streamflow and mean air temperature increase significantly at rates of about 12.30 mm/10a and 0.28 °C/10a during 1979-2013 in the study area. The results of gray relational analysis indicate that the air temperature acts as a primary factor for the increased streamflow. Due to climate warming, the total glacier volume has retreated by over 25% for the past half century, and the areal extent of permafrost has degraded by 15.3% in the recent twenty years. Parallel comparisons with other sub-basins in the Lhasa River Basin indirectly reveal that the increased streamflow at the Yangbajain station is mainly fed by the accelerated glacier retreat. Through baseflow recession analysis, we also find that the estimated groundwater storage that is comparable with the GRACE data increases significantly at the rates of about 19.32 mm/10a during these years. That is to say, as permafrost thawing, more spaces have been released to accommodate the increasing meltwater. The results in this study suggest that due to climate warming the impact of glacial retreat and permafrost degradation shows compound behaviors on storage-discharge mechanism, which fundamentally affects the water supply and the mechanisms of streamflow generation and change.

Keywords: Climate warming; Streamflow; Groundwater storage; Glacier retreat; Permafrost degradation; Tibetan Plateau

1. Introduction

Often referred to as the “Water Tower of Asia”, the Tibetan Plateau (TP) is the source area of major rivers in Asia, e.g., the Yellow, Yangtze, Lancang-Mekong, Yarlu Zangbo-Brahmaputra, and Nu-Salween, Indus Rivers (Cuo et al., 2014). The delayed release of water resources on the TP through glacier melt can augment river runoff during dry periods, giving it a pivotal role for water supply for downstream populations, agriculture and industries in these rivers (Viviroli et al., 2007; Pritchard, 2017). However, the TP is experiencing a significant warming period during the last half century (Kang et al., 2010; Liu and Chen, 2000). Along with the rising temperature, major warming-induced changes have occurred over the TP, such as glacier retreat (Yao et al., 2004; Yao et al., 2007) and frozen ground degradation (Wu and Zhang, 2008; Xu et al., 2019). Hence, it is of great importance to elucidate how climate warming influences hydrological processes and water resources on the TP.

In cold alpine catchments, glacier is known as “solid reservoir” that supplies water through streamflow, while frozen ground, especially permafrost, servers as an impermeable barrier to the interaction between surface water and groundwater (Immerzeel et al., 2010; Walvoord and Kurylyk, 2016; Rogger et al., 2017). Since the 1990s, most glaciers across the TP have retreated rapidly due to global warming and caused an increase of more than 5.5% in river runoff from the plateau (Yao et al., 2007). Meltwater is the key contributor to streamflow increase especially for headwater catchments with larger glacier coverage (>5%) (Bibi et al., 2018; Xu et al.,

2019). For example, the total discharge increase by 2.7%-22.4% mainly due to increased glacier melt that accounts for more than half of the total discharge increase in the upper Brahmaputra, i.e., Yarlu Zangbo (Su et al., 2016).

Meanwhile, in a warming climate, numerous studies suggested that frozen ground on the TP has experienced a noticeable degradation during the past decades (Cheng and Wu, 2007; Wu and Zhang, 2008; Zou et al., 2017). Frozen ground degradation can modify surface conditions and change thawed active layer storage capacity in the alpine catchments (Niu et al., 2011). Thawing of frozen ground increases surface water infiltration, supports deeper groundwater flow paths, and then enlarges groundwater storage, which is expected to have a profound effect on flow regimes (Kooi et al., 2009; Bense et al., 2012; Walvoord and Striegl, 2007; Woo et al., 2008; Ge et al., 2011; Walvoord and Kurylyk, 2016). For example, Walvoord and Striegl (2007) found that permafrost thawing in an arctic basin has resulted in a general upwards trend in groundwater contribution to streamflow of 0.7-0.9%/yr, however, with no pervasive change in total annual runoff. Similar results have also been found in the central and northern TP (Liu et al., 2011; Niu et al., 2016; Xu et al., 2019). Moreover, a slowdown in baseflow recession was found in the northeastern and central TP (Niu et al., 2011; Niu et al., 2016; Wang et al., 2017), in northeastern China (Duan et al., 2017), and in Arctic rivers (Lyon et al., 2009; Lyon and Destouni, 2010; Walvoord and Kurylyk, 2016).

Generally, in alpine regions, climate warming by triggering glacier retreat and

permafrost thawing is changing hydrological processes of storage and discharge. However, direct measurement of the changing of permafrost depth or catchment aquifer storage is still difficult to perform at catchment scale (Xu et al., 2019; Staudinger, 2017; Käser and Hunkeler, 2016). Though its resolution and accuracy is relatively low, GRACE data has always been adopted in assessing total groundwater storage changes (Green et al., 2011). Quantitatively characterizing storage properties and sensitivity to climate warming in cold alpine catchments is desired for local water as well as downstream water management (Staudinger, 2017).

Xu et al. (2019) used a simple ratio of the maximum and minimum runoff to indirectly indicate the change of storage capacity as well as the effects of permafrost on recession processes. An alternative method, namely, recession flow analysis, can theoretically be used to derive the active groundwater storage volume to reflect frozen ground degradation in a catchment (Brutsaert and Nieber, 1977; Brutsaert, 2008). For example, the groundwater storage changes can be inferred by recession flow analysis assuming linearized outflow from aquifers into streams (Lin and Yeh, 2017). Due to the complex structures and properties of catchment aquifers, the linear reservoir model may not sufficient to represent the actual storage dynamics (Wittenberg, 1999; Chapman, 1999; Liu et al., 2016). Hence, Lyon et al. (2009) adopted the nonlinear reservoir to fit baseflow recession curves for the derivation of aquifer attributes, which can be developed for inferring aquifer storage. Buttle (2017) used Kirchner's (2009) approach for estimating the dynamic storage in different basins and found that

101 the storage and release of dynamic storage may mediate baseflow response to
102 temporal changes. Generally, the classical recession flow analysis that is based on
103 widely easily available hydrologic data is still widely used to provide important
104 information on storage–discharge relationship of the basin (Patnaik et al., 2018).

105 In this study, the Yangbajain Catchment in the Lhasa River Basin is adopted as the
106 study area. The catchment is experiencing glacier retreat and frozen ground
107 degradation in response to climate warming. The main objectives of this study are (1)
108 to assess the changes between surface runoff and baseflow in a warming climate; (2)
109 to quantify active groundwater storage volume by recession flow analysis; (3) to
110 analyze the impacts of the changes in active groundwater storage on streamflow
111 variation. The paper is structured as follows. The section of Materials and Methods
112 includes the study area, data sources and methods. The Results and Discussion
113 sections present the changes in streamflow and its components, climate factors, and
114 glaciers, and we will discuss the changing regimes of streamflow volume and
115 baseflow recession in response to the changes of active groundwater storage and
116 glaciers. The main conclusions are summarized in the section of Conclusions.

117 **2. Materials and Methods**

118 **2.1. Study area**

119 The 2,645 km^2 Yangbajain Catchment in the western part of the Lhasa River Basin
120 (Figure 1a) lies between the Nyainqêntanglha Range to the northwest and the
121 Yarlu-Zangbo suture to the south. In the central of the catchment, a wide and flat

122 valley (Figure 1b) with low-lying terrain and thicker aquifers is in a half-graben
123 fault-depression basin caused by the Damxung-Yangbajain Fault (Wu and Zhao, 2006;
124 Yang et al., 2017). As a half graben system, the north-south trending
125 Damxung-Yangbajain Fault (Figure 1b) provides the access for groundwater flow as
126 manifested by the widespread distribution of hot springs (Jiang et al., 2016). The
127 surface of the valley is blanketed by Holocene-aged colluvium, filled with the great
128 thickness of alluvial-pluvial sediments from the south such as gravel, sandy loam, and
129 clay. The vegetation in the catchment is characterized by alpine meadow, alpine
130 steppe, marsh, shrub, etc, and meadow and marsh are mainly distributed in the valley
131 and river source (Zhang et al., 2010).

132 Located on the south-central TP, the Yangbajain Catchment is a glacier-fed
133 headwater catchment with significant frozen ground coverage (Figures 1b & 1c). A
134 majority of glaciers were found along the Nyainqêntanglha Ranges (Figure 1b).
135 Glaciers cover over ten percent of the whole catchment, making it the most
136 glacierized sub-basin in the Lhasa River Basin. According to the First Chinese Glacier
137 Inventory (Mi et al., 2002), the total glacier area was about 316.31 km^2 in 1960. The
138 ablation period of the glaciers ranges from June to September with the glacier termini
139 at about 5,200 m (Liu et al., 2011). According to the new map of permafrost
140 distribution on the TP (Zou et al., 2017), the valley is underlain by seasonally frozen
141 ground (Figure 1c). It is estimated that seasonally frozen ground and permafrost
142 accounts for about 64% and 36% of the total catchment area, respectively (Zou et al.,

2017). The lower limit of alpine permafrost is around 4,800 m, and the thickness of permafrost varies from 5 m to 100 m (Zhou et al., 2000).

The catchment is characterized by a semi-arid temperate monsoon climate. The areal average annual air temperature of the Yangbajain Catchment is approximately -2.3°C with monthly variation from -8.6°C in January to 3.1°C in July (Figure 2). The average annual precipitation at the Yangbajain Station is about 427 mm. The catchment has a summer (June-August) monsoon with 73% of the yearly precipitation, while the rest of the year is dry with only 1% of the yearly precipitation occurring in winter (December-February) (Figure 2).

The average annual streamflow at the Yangbajain Station is 277.7 mm, and the intra-annual distribution of streamflow is uneven (Figure 2). In summer, streamflow is recharged mainly by monsoon rainfall and meltwater, and the volume of summer runoff accounts for approximately 63% of the yearly streamflow (Figure 2). The streamflow in winter with only 4% of the yearly streamflow (Figure 2) is only recharged by groundwater, which is greatly affected by the freeze-thawing cycle of frozen ground and the active layer (Liu et al., 2011).

2.2. Data

Daily streamflow and precipitation data at four hydrological Stations (Figure 1a) during the period 1979-2013 are collected from the Tibet Autonomous Region Hydrology and Water Resources Survey Bureau. The monthly meteorological data at three weather stations (Figure 1a) are obtained from the China Meteorological Data

Sharing Service System (http://data.cma.cn/) for the years from 1979 to 2013. In this study, the method of meteorological data extrapolation by Prasch et al. (2013) is adopted to obtain the discretisized air temperature (with cell size as 1 km×1 km) of the Lhasa River Basin based on the air temperature of the three stations assuming a linear lapse rate. The mean monthly lapse rate is set to 0.44 °C/100m for elevations below 4,965 m and 0.78 °C/100m for elevations above 4,965 m in the catchment (Wang et al., 2015).

The glaciers and frozen ground data are provided by the Cold and Arid Regions Science Data Center (http://westdc.westgis.ac.cn/). The distribution, area and volume of glaciers are based on the First and Second Chinese Glacier Inventory in 1960 and 2009 (Mi et al., 2002; Liu et al., 2014) (Figure 1b). The distribution and classification of frozen ground (Figure 1c) are collected from the twice maps of frozen ground on the TP (Li and Cheng, 1996; Zou et al., 2017).

The latest Level□3 monthly mascon solutions (CSR, Save et al., 2016) was used to detect terrestrial water storage (TWS, total vertically-integrated water storage) changes for the period from January 2003 to December 2015 with spatial sampling of 0.5°×0.5° from the Gravity Recovery and Climate Experiment (GRACE) satellite. The time series of 2003~2015 for snow water equivalent (SWE), total soil moisture (SM, layer 0~200cm) from the dataset (GLDAS_Noah2.1, https://disc.gsfc.nasa.gov/) were adopted for derivation of the groundwater storage (GWS) (Richey et al., 2015).

2.3. Methods

185 *2.3.1. Statistical methods for assessing streamflow changes*

186 The Mann-Kendall (MK) test, which is suitable for data with non-normally
187 distributed or nonlinear trends, is applied to detect trends of hydro-meteorological
188 time series (Mann, 1945; Kendall, 1975). To remove the serial correlation from the
189 examined time series, a Trend-Free Pre-Whitening (TFPW) procedure is needed prior
190 to applying the MK test (Yue et al., 2002). A more detailed description of the
191 Trend-Free Pre-Whitening (TFPW) approach was provided by Yue et al. (2002).

192 Gray relational analysis was aimed to find the major climatic or hydrological
193 factors that influenced an objective variable (Liu et al., 2005; Wang et al., 2013). In
194 this paper, gray relational analysis is used to investigate the main climatic factors
195 impacting the streamflow.

196 *2.3.2. Baseflow separation*

197 In this paper, the most widely used one-parameter digital filtering algorithm is
198 adopted for baseflow separation (Lyne and Hollick, 1979). The filter equation is
199 expressed as

200 $$q_t = \alpha q_{t-1} + \frac{1+\alpha}{2}\left(Q_t - Q_{t-1}\right) \quad (1)$$

201 $$b_t = Q_t - q_t \quad (2)$$

202 where q_t and q_{t-1} are the filtered quick flow at time step t and t-1, respectively; Q_t and
203 Q_{t-1} are the total runoff at time step t and t-1; α is the filter parameter that ranging
204 from 0.9 to 0.95; b_t is the filtered baseflow.

205 *2.3.3. Determination of active groundwater storage*

206 In this study, the active groundwater storage (also abbreviated as groundwater
207 storage in the following context) is assumed as a storage that directly controls
208 streamflow dynamics during rainless periods (Kirchner, 2009; Staudinger, 2017).
209 Based on hydraulic groundwater theory, groundwater storage in a catchment can be
210 approximated as a power function of baseflow rate at the catchment outlet (Brutsaert,
211 2008).

212 $$S = Ky^m \tag{8}$$

213 where y is the rate of baseflow in the stream, and S is the volume of active
214 groundwater storage in the catchment aquifers (see in Figure 3). Here K, m are
215 constants depending on the catchment physical characteristics, and K is the baseflow
216 recession coefficient, which represents the time scale of the catchment streamflow
217 recession process.

218 During dry season without precipitation and other input events, the conservation of
219 mass equation can be represented as

220 $$\frac{dS}{dt} = -y \tag{9}$$

221 where t is the time. Substitution of equation (8) in equation (9) yields (Brutsaert and
222 Nieber, 1977)

223 $$-\frac{dy}{dt} = ay^b \tag{10}$$

224 where dy/dt is the temporal change of the baseflow rate during recessions, and the
225 constants a and b are called the recession intercept and recession slope of plots of
226 $-dy/dt$ versus y in log-log space, respectively. In the storage discharge relationship,

227 the aquifer responds as a linear reservoir if b=1, and as nonlinear reservoir if b≠1. In
228 addition, with a fixed slope b, the changes in catchment aquifer properties by fitting
229 the intercept a as a variable ban be observed (Rupp and Selker, 2006).

230 According to Gao et al. (2017), the parameters of K and m in equation (8) can be
231 expressed by a and b, where $K=1/\left[a\left(2-b\right)\right]$ and $m=2-b$. Furthermore, the
232 constants a and b can be determined through the technique of recession slope curves.
233 In this study, the two constants are curve-fitted by using a nonlinear least squares
234 regression through all data points of $-dy/dt$ versus y in log-log space for all years to
235 avoid the difficulty of defining a lower envelop of the scattered points (Lyon et al.,
236 2009). According to the values of a and b, K and m can be calculated. Thus the
237 average groundwater storage S for dry season can be obtained through equation (8)
238 based on average rate of baseflow.

239 **3. Results**

240 **3.1. Assessment of streamflow changes**

241 The annual streamflow of the Yangbajain Catchment shows an increasing trend at
242 the 5% significance level with a mean rate of about 12.30 mm/10a over the period
243 1979-2013 (Table 1 and Figure 4a). Meanwhile, annual mean air temperature exhibits
244 an increasing trend at the 1% significance level with a mean rate of about 0.28 °C/10a
245 (Table 1 and Figure 5a). However, annual precipitation has a nonsignificant trend
246 during this period (Table 1 and Figure 5b).

247 As annual streamflow increases significantly, it is necessary to analyze to what

248 extent the changes in the two components (quick flow and baseflow) lead to
249 streamflow increases. Based on the baseflow separation method, the annual mean
250 baseflow contributes about 59% of the annual mean streamflow in the catchment. The
251 MK test shows that annual baseflow exhibits a significant increasing trend at the 1%
252 level with a mean rate of about 10.95 mm/10a over the period 1979-2013 (Table 1 and
253 Figure 4b). But the trend is statistically nonsignificant for annual quick flow in the
254 same period (Table 1). The increasing trends between the baseflow and streamflow
255 are very close, indicating that the increase in baseflow is the main contributor to
256 streamflow increases.

257 Furthermore, gray relational analysis is applied to the catchment to identify the
258 major climatic factors for the increasing streamflow. The result shows that the air
259 temperature has the higher gray relational grade at annual scale (Table 2). This
260 indicates that the air temperature acts as a primary factor for the increased streamflow
261 as well as the baseflow.

262 The annual streamflow and baseflow significantly increase due to the rising air
263 temperature over the period 1979-2013. However, there are diverse intra-annual
264 variation characteristics for streamflow as well as the two streamflow components
265 during the period. Streamflow in spring (March to May), autumn (September to
266 November) and winter (December to February) show increasing trends at least at the
267 5% significance level (Figure 6a, 6c and 6d), while streamflow in summer (June to
268 August) has a nonsignificant trend during this period (Figure 6b). Baseflow also

increases significantly in spring, autumn and winter (Figure 6a, 6c and 6d). The trend is statistically nonsignificant for baseflow in summer (Figure 6b). Quick flow exhibits nonsignificant trend for all seasons (Table 1). As to the meteorological factors, mean air temperature in all seasons increase significantly at the 1% level especially during winter with the rate of about 0.51°C/10a (Table 1 and Figure 7), whereas precipitation in each season shows nonsignificant trend during these years (Table 1). The gray relational analysis shows that the air temperature is the critical climatic factor for the changes in streamflow and baseflow in all seasons (Table 2).

3.2. Estimation of groundwater storage by baseflow recession analysis

Daily streamflow and precipitation records in autumn and early winter (September to December) was adopted. In this dry season, hydrograph usually with little precipitation declines consecutively and smoothly. The fitted slope b is equal to 1.79 through the nonlinear least square fit of equation (10) for all data points of $-dy/dt$ versus y in log-log space during the period 1979-2013. Moreover, for each decade or year, the intercept a could be fitted by the fixed slope b=1.79. Then, the values of K and m for each decade or year can be determined. And the groundwater storage S for each year can be directly estimated from the average rate of baseflow during a recession period through equation (8).

Figure 8 shows the results of the nonlinear least square fit for each decade's recession data from the 1980s, 1990s and 2000s, respectively. As shown in Figure 8, the recession data points and fitted recession curves of each decade gradually move

290 downward as time goes on. This indicates that, with a fixed slope *b*, the intercept *a*
291 gradually decreases and recession coefficient *K* increases accordingly. The values of
292 recession coefficient *K* for each decade are 77 $mm^{0.79}d^{0.21}$, 84 $mm^{0.79}d^{0.21}$ and 103
293 $mm^{0.79}d^{0.21}$. Furthermore, Figure 9a shows the inter-annual variation of recession
294 coefficient *K* during the period 1979-2013. In total, though there are some large
295 fluctuations or even a rather large decrease at the beginning of the 1990s, the overall
296 increasing trend of 7.70 ($mm^{0.79}d^{0.21}$)/10a at a significance level of 5% is similar to the
297 results obtained from decade analysis. This long-term variation of recession
298 coefficient *K* from September to December indicates that baseflow recession during
299 autumn and early winter gradually slows down in the catchment.

300 According to the results of decade data fit (see in Figure 8), the mean values of
301 groundwater storage *S* estimated for each decade are 130 mm, 148 mm and 188 mm
302 for the 1980s, 1990s and 2000s. The inter-annual variation of groundwater storage *S*
303 is also similar with recession coefficient *K* (Figure 9a and 9b). The decreased trend of
304 anomalies changes of groundwater storage (*GWS*) estimated by the GRACE data is
305 consistent with the annual trend of *S* during 2003~2015 (Figure 9b). And the reduced
306 volume of groundwater between *GWS* and *S* are also comparable (~100-120 mm),
307 which has partly verified our estimations.

308 The trend analysis suggests that the groundwater storage *S* shows an increasing
309 trend at the 5% significance level with a rate of about 19.32 mm/10a during the period
310 1979-2013 (Figure 9b). The annual trend of groundwater storage *S* from 1979 to 2013

311 is consistent with the values across decades. This indicates that groundwater storage
312 has been enlarged. Through recent field investigations, we know that groundwater
313 level is rising. The increases of surface water and shallow groundwater storages are
314 changing the land cover. For example the Normalized Difference Vegetation Index
315 (NDVI) is rising accordingly in the past twenty years (Figure 10). In fact, not only in
316 the study area but in the whole TP, surface water and groundwater storage are
317 increasing due to climate warming, and hence vegetation conditions have been
318 improved (Zhang et al., 2018; Khadka et al., 2018).

319 **4. Discussions**

320 The results have revealed that the increase of streamflow especially in dry season is
321 tightly related with climate warming. It is obviously that both glacier retreat and
322 frozen ground degradation in a warmer climate can significantly alter the mechanism
323 of streamflow. In the Yangbajain Catchment as well as the whole Lhasa River Basin,
324 it is experiencing a noticeable glacier retreat and frozen ground degradation during the
325 past decades (Table 3). For instance, according to the twice map of frozen ground
326 distribution on the TP (Li and Cheng, 1996; Zou et al., 2017), the areal extent of
327 permafrost in the Yangbajain catchment has decreased by 406 km^2 (15.3%) over the
328 past 22 years; the areal extent of seasonal frozen ground has increased by 406 km^2
329 (15.3%) with the corresponding degradation of permafrost.

330 According to the new map of permafrost distribution on the Tibetan Plateau (Zou et
331 al., 2017), the coverages of permafrost and seasonally frozen ground in each

sub-catchment (especially the Lhasa sub-catchments) are comparable to that in the Yangbajain Catchment; but the coverage of glaciers in the three catchments is far lower than that in the Yangbajain Catchment according to the First Chinese Glacier Inventory (Mi et al., 2002) (Table 3). The MK test showed that, in all the four catchments, the annual mean air temperature had significant increases at the 1% significance level (Figure 4) while the annual precipitation showed nonsignificant trends (Table 4). The annual streamflow of the three Lhasa, Pangdo and Tangga Catchments all had nonsignificant trends, while the annual streamflow of the Yangbajain Catchment showed an increasing trend at the 5% significance level with a mean rate of about 12.30 mm/10a during the period. Ye et al. (1999) stated that when glacier coverage is greater than 5%, glacier contribution to streamflow induced by climate warming starts to show up. As reported by Prasch et al. (2013), the contribution of accelerated glacial meltwater to streamflow would bring a significant increase in streamflow in the Yangbajain Catchment. Thus it is reasonable to attribute annual streamflow increases to the accelerated glacier retreat as the consequence of increasing annual air temperature.

Although permafrost degradation is not the controlling factor for the increase of streamflow, a rational hypothesis is that increased groundwater storage S in autumn and early winter is associated with frozen ground degradation, which can enlarge groundwater storage capacity (Niu et al., 2016). Figure 3 depicts the changes of surface flow and groundwater flow paths in a glacier fed catchment, which is

353 underlain by frozen ground under past climate and warmer climate, respectively. As
354 frozen ground extent continues to decline and active layer thickness continues to
355 increase in the valley, the enlargement of groundwater storage capacity can provide
356 enough storage space to accommodate the increasing meltwater that may percolate
357 into deeper aquifers (Figure 3). Then, the increase of groundwater storage in autumn
358 and early winter allows more groundwater discharge into streams as baseflow, and
359 lengthens the recession time as indicated by recession coefficient *K*. This leads to the
360 increased baseflow and slow baseflow recession in autumn and early winter, as is
361 shown in Figure 6c, 6d and Figure 9a. In the late winter and spring, the increase of
362 baseflow (Figure 6d and 6a) can be explained by the delayed release of increased
363 groundwater storage.

364 Thus, as the results of climate warming, river regime in this catchment has been
365 altered significantly. On the one hand, permafrost degradation is changing the aquifer
366 structure that controls the storage-discharge mechanism, e.g., catchment groundwater
367 storage increases at about 19.32 mm/10a. On the other hand, huge amount of water
368 from glacier retreat is contributing to the increase of streamflow and groundwater
369 storage. For example, the annual streamflow of the Yangbajain Catchment increases
370 with a mean rate of about 12.30 mm/10a during the past 50 years. However, the total
371 glacial area and volume have decreased by 38.05 km^2 (12.0%) and 1788 mm (26.2%)
372 over the period 1960-2009 (Figure 11) according to the Chinese Glacier Inventories.
373 Hence, the reduction rate of glacial volume is 9.46×10^7 m^3/a (about 357.7 mm/10a) on

374 average during the past 50 years. In the ablation on continental type glaciers in China,
375 evaporation (sublimation) always takes an important role, however, annul amount of
376 evaporation is usually less than 30% of the total ablation of glaciers in the high
377 mountains of China (Zhang et al., 1996). Given the 30% reduction in glacial melt,
378 there is still a large water imbalance between melt-derived runoff and the actually
379 increase of runoff and groundwater storage. Our results imply that more than 60% of
380 glacial meltwater would be lost by subsurface leakage.

381 **5. Conclusions**

382 In this study, the changes of hydro-meteorological variables were evaluated to
383 identify the main climatic factor for streamflow changes in the cryospheric
384 Yangbajain Catchment. We find that the annual streamflow especially the annual
385 baseflow increases significantly, and the rising air temperature acts as a primary factor
386 for the increased runoff. Furthermore, through parallel comparisons of sub-basins in
387 the Lhasa River Basin, we indirectly presumed that the increased streamflow in the
388 Yangbajain catchment is mainly fed by glacier retreat. Due to the climate warming,
389 the total glacial area and volume have decreased by 38.05 km^2 (12.0%) and 4.73×10^9
390 m^3 (26.2%) in 1960-2009, and the areal extent of permafrost has degraded by 406 km^2
391 (15.3%) in the past 22 years. As a results of permafrost degradation, groundwater
392 storage capacity has been enlarged, which triggers a continuous increase of
393 groundwater storage at a rate of about 19.32 mm/10a. This can explain why baseflow
394 volume increases and baseflow recession slows down in autumn and early winter.

At last we find that there is a large water imbalance (> 5.79×10^7 m^3/a) between melt-derived runoff and the actually increase of runoff and groundwater storage, which suggests more than 60% of the reduction in glacial melt should be lost by subsurface leakage. However, the pathway of these leakage is still an open question for further studies. More methods (e.g., hydrological isotopes) should be adopted to quantify the contribution of glaciers meltwater and permafrost degradation to streamflow, and to explore the change of groundwater storage capacity as frozen ground continues to degrade.

Acknowledgements:

This work was supported by the National Natural Science Foundation of China (NSFC) (grants 91647108, 91747203), the Science and Technology Program of Tibet Autonomous Region (2015XZ01432), the West Light Foundation of the Chinese Academy of Sciences (29Y929621) and the Special Fund of the State Key Laboratory of Hydrology-Water Resources and Hydraulic Engineering (no 20185044312).

References

Kooi, H., Ferguson, G., Bense, V. F.: Evolution of shallow groundwater flow systems in areas of degrading permafrost, Geophysical Research Letters, 36(22):297-304, 2009.

Bense, V. F., Kooi, H., Ferguson, G., and Read, T.: Permafrost degradation as a control on hydrogeological regime shifts in a warming climate, Journal of Geophysical Research Earth Surface, 117, F03036, doi:10.1029/2011JF002143, 2012.

Bibi, S., Wang, L., Li, X. P., Zhou, J., Chen, D. L., and Yao, T. D.: Climatic and associated cryospheric, biospheric, and hydrological changes on the Tibetan Plateau: A review, International Journal of Climatology, 38, e1-e17, doi:10.1002/joc.5411, 2018.

Brutsaert, W., and Lopez, J. P.: Basin-scale geohydrologic drought flow features of riparian aquifers in the southern Great Plains, Water Resources Research, 34(2), 233-240, 1998.

Brutsaert, W., and Nieber, J. L.: Regionalized drought flow hydrographs from a mature glaciated plateau, Water Resources Research, 13(3), 637-643, 1977.

Brutsaert, W.: Long-term groundwater storage trends estimated from streamflow records: Climatic perspective, Water Resources Research, 44(2), 114-125, doi:10.1029/2007WR006518, 2008.

Buttle, J. M.: Mediating stream baseflow response to climate change: the role of basin storage, Hydrological Processes, 32(1), doi:10.1002/hyp.11418, 2017.

Chapman, T.: A comparison of algorithms for stream flow recession and baseflow separation, Hydrological Processes, 13, 701-714, 1999.

Cheng, G. D., and Wu, T. H.: Responses of permafrost to climate change and their environmental significance, Qinghai-Tibet Plateau, Journal of Geophysical Research Earth Surface, 112, F02S03, doi:10.1029/2006JF000631, 2007.

Cuo, L., Zhang, Y. X., Zhu, F. X., and Liang, L. Q.: Characteristics and changes of streamflow on the Tibetan Plateau: A review, Journal of Hydrology Regional Studies, 2, 49-68, doi:10.1016/j.ejrh.2014.08.004, 2014.

Ding, Y. J., Zhang. S.Q., and Chen, R. S.: Introduction to hydrology in cold regions, Science Press, Beijing, China, 2017. (In Chinese).

Duan, L., Man, X., Kurylyk, B.L., Cai, T.: Increasing winter baseflow in response to permafrost thaw and precipitation regime shifts in northeastern China, Water, 9, 25, doi:10.3390/w9010025, 2017.

444 Evans, S. G., and Ge, S.: Contrasting hydrogeologic responses to warming in
445 permafrost and seasonally frozen ground hillslopes, Geophysical Research Letters,
446 44, 1803-1813, doi:10.1002/2016GL072009, 2017.
447 Gao, M., Chen, X., Liu, J., Zhang, Z., and Cheng, Q.: Using two parallel linear
448 reservoirs to express multiple relations of power-law recession curves, Journal of
449 Hydrologic Engineering, 04017013, doi:10.1061/(ASCE)HE.1943-5584.0001518,
450 2017.
451 Ge, S., J. McKenzie, C. Voss, and Wu, Q.: Exchange of groundwater and
452 surface-water mediated by permafrost response to seasonal and long term air
453 temperature variation, Geophysical Research Letters, 38, L14402,
454 doi:10.1029/2011GL047911, 2011.
455 Green, T. R., Taniguchi, M., Kooi, H., Gurdak, J. J., Allen, D. M., and Hiscock, K. M.,
456 et al.: Beneath the surface of global change: impacts of climate change on
457 groundwater, Journal of Hydrology, 405(3), 532-560,
458 doi:10.1016/j.jhydrol.2011.05.002, 2011.
459 Immerzeel, W. W., van Beek, L. P. H., and Bierkens, M. F. P.: Climate change will
460 affect the Asian water towers, Science, 328, 1382-1385, 2010.
461 Jiang, W., Han, Z., Zhang, J., and Jiao, Q.: Stream profile analysis, tectonic
462 geomorphology and neotectonic activity of the Damxung-Yangbajain Rift in the
463 south Tibetan Plateau, Earth Surface Processes and Landforms, 41(10), 1312-1326,
464 doi:10.1002/esp.3899, 2016.
465 Kang, S. C., Xu, Y. W., You, Q. L., Flügel, W. A., Pepin, N., and Yao, T. D.: Review of
466 climate and cryospheric change in the Tibetan Plateau, Environmental Research
467 Letters, 5(1), 015101, doi:10.1088/1748-9326/5/1/015101, 2010.
468 Käser, D., and D. Hunkeler.: Contribution of alluvial groundwater to the outflow of
469 mountainous catchments, Water Resources Research, 52, 680-697,
470 doi:10.1002/2014WR016730, 2016.

Kendall, M. G.: Rank Correlation Methods, 4th ed, Charles Griffin, London, pp. 196, 1975.

Khadka, N., Zhang, G., and Thakuri, S.: Glacial Lakes in the Nepal Himalaya: Inventory and Decadal Dynamics (1977–2017). Remote Sensing, 10, 1913, doi:10.3390/rs10121913, 2018.

Kirchner, J.W.: Catchments as simple dynamical systems: catchment characterization, rainfall-runoff modeling, and doing hydrology backward, Water Resources Research, 45, W02429, doi:10.1029/2008WR006912, 2009.

Li, S., and Cheng, G.: Map of Frozen Ground on Qinghai-Xizang Plateau, Gansu Culture Press, Lanzhou, 1996.

Lin, K. T., and Yeh, H. F.: Baseflow recession characterization and groundwater storage trends in northern Taiwan, Hydrology Research, 48(6), 1745-1756, 2017.

Liu, J. S., Xie, J., Gong, T. L., Wang, D., and Xie, Y. H.: Impacts of winter warming and permafrost degradation on water variability, upper Lhasa River, Tibet, Quaternary International, 244(2), 178-184, doi:10.1016/j.quaint.2010.12.018, 2011.

Liu, J. T., Han, X. L., Chen, X., Lin, H., and Wang, A. H.: How well can the subsurface storage-discharge relation be interpreted and predicted using the geometric factors in headwater areas? Hydrological Processes, 30(25), 4826-4840, doi:10.1002/hyp.10958, 2016.

Liu, Q. Q, Singh, V. P., and Xiang, H.: Plot erosion model using gray relational analysis method, Journal of Hydrologic Engineering, 10, 288-294, 2005.

Liu, S. Y., Guo, W., and Xu, J., et al.: The Second Glacier Inventory Dataset of China (Version 1.0), Cold and Arid Regions Science Data Center at Lanzhou, 2014, doi:10.3972/glacier.001.2013.db.

Liu, X. D., and Chen, B. D.: Climatic warming in the Tibetan Plateau during recent decades, International Journal of Climatology, 20(14), 1729-1742, 2000.

Lyne, V., and Hollick, M.: Stochastic time-variable rainfall-runoff modeling, Aust.

Natl. Conf. Publ. pp.89-93, 1979.

Lyon, S. W., and Destouni, G.: Changes in catchment-scale recession flow properties in response to permafrost thawing in the Yukon River basin, International Journal of Climatology, 30(14), 2138-2145, doi:10.1002/joc.1993, 2010.

Lyon, S. W., Destouni, G., Giesler, R., Humborg, C., Mörth, M., and Seibert, J., et al.: Estimation of permafrost thawing rates in a sub-arctic catchment using recession flow analysis, Hydrology and Earth System Sciences, 13(5), 595-604, 2009.

Mann, H.: Non-parametric test against trend, Econometrica, 13, 245-259, 1945.

Mi, D. S., Xie, Z. C., and Luo, X. R.: Glacier Inventory of China (volume XI: Ganga River drainage basin and volume XII: Indus River drainage basin). Xi'an Cartographic Publishing House, Xi'an, pp. 292-317, 2002 (In Chinese).

Niu, L., Ye, B. S., Li, J., and Sheng, Y.: Effect of permafrost degradation on hydrological processes in typical basins with various permafrost coverage in western China, Science China Earth Sciences, 54(4), 615-624, doi:10.1007/s11430-010-4073-1, 2011.

Niu, L., Ye, B., Ding, Y., Li, J., Zhang, Y., Sheng, Y., and Yue, G.: Response of hydrological processes to permafrost degradation from 1980 to 2009 in the upper Yellow River basin, China, Hydrology Research, 47(5), 1014-1024, doi:10.2166/nh.2016.096, 2016.

Patnaik, S., Biswal1, B., Kumar, D. N., Sivakumar, B.: Regional variation of recession flow power□law exponent, Hydrological Processes, 32, 866–872, 2018.

Prasch, M., Mauser, W., and Weber, M.: Quantifying present and future glacier melt-water contribution to runoff in a central Himalayan river basin, Cryosphere, 7(3), 889-904, doi:10.5194/tc-7-889-2013, 2013.

Pritchard, H. D.: Asia's glaciers are a regionally important buffer against drought, Nature, 545(7653), 169, doi:10.1038/nature22062, 2017.

Richey, A. S., Thomas, B. F., Lo, M.-H., Reager, J. T., Famiglietti, J. S., Voss, K.,

525 Swenson, S., and Rodell, M.: Quantifying renewable groundwater stress with
526 GRACE, Water Resources Research, 51, 5217–5238, doi:10.1002/ 2015WR017349,
527 2015.
528 Rogger, M., Chirico, G. B., Hausmann, H. Krainer, K. Brückl, E. Stadler, P. and
529 Blöschl, G.: Impact of mountain permafrost on flow path and runoff response in a
530 high alpine catchment, Water Resources Research, 53, 1288-1308, doi:10.1002/
531 2016WR019341, 2017.
532 Rupp, D. E., and Selker, J. S.: Information, artifacts, and noise in d*Q*/d*t*-*Q* recession
533 analysis, Advances in Water Resources, 29(2), 154-160, 2006.
534 Save, H., Bettadpur, S., and Tapley, B. D.: High□resolution CSR GRACE RL05
535 masons, Journal of Geophysical Research: Solid Earth, 121, 7547–7569,
536 doi.org/10.1002/2016JB013007, 2016.
537 Staudinger, M., Stoelzle, M., Seeger, S., Seibert, J., Weiler, M., and Stahl, K.:
538 Catchment water storage variation with elevation, Hydrological Processes, 31(11),
539 doi:10.1002/hyp.11158, 2017.
540 Su, F., Zhang, L., Ou, T., Chen, D., Yao, T., Tong, K., and Qi, Y.: Hydrological
541 response to future climate changes for the major upstream river basins in the
542 Tibetan Plateau. Global and Planetary Change, 136, 82-95, doi:10.1016/j.gloplacha.
543 2015.10.012, 2016.
544 Viviroli, D., Du¨rr, H. H., Messerli, B., Meybeck, M., and Weingartner, R.: Mountains
545 of the world, water towers for humanity: Typology, mapping, and global
546 significance, Water Resources Research, 43, W07447, doi:10.1029/2006WR005653,
547 2007.
548 Walvoord, M. A., and Kurylyk, B. L.: Hydrologic impacts of thawing permafrost-A
549 review, Vadose Zone Journal, 15(6), doi:10.2136/vzj2016.01.0010, 2016.
550 Walvoord, M. A., and Striegl, R. G.: Increased groundwater to stream discharge from
551 permafrost thawing in the Yukon River basin: Potential impacts on lateral export of

carbon and nitrogen, Geophysical Research Letters, 34(12), 123-134, doi:10.1029/2007GL030216, 2007.

Wang, G., Mao, T., Chang, J., Song, C., and Huang, K.: Processes of runoff generation operating during the spring and autumn seasons in a permafrost catchment on semi-arid plateaus, Journal of Hydrology, 550, 307-317, 2017.

Wang, S., Liu, S. X., Mo, X. G., Peng, B., Qiu, J. X., Li, M. X., Liu, C. M., Wang, Z. G., and Bauer-Gottwein, P.: Evaluation of remotely sensed precipitation and its performance for streamflow simulations in basins of the southeast Tibetan Plateau, Journal of Hydrometeorology, 16(6), 342-354, doi:10.1175/JHM-D-14-0166.1, 2015.

Wang, Y. F., Shen, Y. J., Chen, Y. N., and Guo, Y.: Vegetation dynamics and their response to hydroclimatic factors in the Tarim River Basin, China, Ecohydrology, 6(6), 927-936, 2013.

Wittenberg, H.: Baseflow recession and recharge as nonlinear storage processes, Hydrological Processes, 13, 715-726, 1999.

Woo, M. K., Kane, D. L., Carey, S. K., and Yang, D.: Progress in permafrost hydrology in the new millennium, Permafrost & Periglacial Processes, 19(2), 237-254, doi:10.1002/ppp.613, 2008.

Wu, Q. B., and Zhang, T. J.: Recent permafrost warming on the Qinghai-Tibetan Plateau, Journal of Geophysical Research Atmospheres, 113, D13108, doi:10.1029/2007JD009539, 2008.

Wu, Z. H., and Zhao, X. T.: Quaternary geology and faulting in the Damxung-Yangbajain Basin, southern Tibet, Journal of Geomechanics, 12(3), 305-316, 2006 (in Chinese).

Xu, M., Kang, S., Wang, X., Pepin, N., and Wu H.: Understanding changes in the water budget driven by climate change in cryospheric-dominated watershed of the northeast Tibetan Plateau, China, Hydrological Processes, 1-19, doi:10.1002/hyp.

13383, 2019.

Yang, G., Lei, D., Hu, Q., Cai, Y., and Wu, J.: Cumulative coulomb stress changes in the basin-range region of Gulu-Damxung-Yangbajain and their effects on strong earthquakes, Electronic Journal of Geotechnical Engineering, 22(5), 1523-1530, 2017.

Yao, T. D., Pu, J. C., Lu, A. X., Wang, Y. Q., and Yu, W. S.: Recent glacial retreat and its impact on hydrological processes on the Tibetan Plateau, China, and surrounding regions, Arctic, Antarctic, and Alpine Research, 39(4), 642-650, 2007.

Yao, T. D., Wang, Y. Q., Liu, S. Y., Pu, J. C., Shen, Y. P., and Lu, A. X.: Recent glacial retreat in high Asia in China and its impact on water resource in northwest China, Science in China, 47(12), 1065-1075, doi:10.1360/03yd0256, 2004.

Ye, B. S., Han, T. D., Ding, Y. J.: Some Changing Characteristics of Glacier Streamflow in Northwest China, Journal of Glaciolgy and Geocryology, 21(1):54-58, 1999 (in Chinese).

Yue, S., Pilon, P., Phinney, B., and Cavadias, G.: The influence of autocorrelation on the ability to detect trend in hydrological series, Hydrological Processes, 16(9), 1807-1829, doi:10.1002/hyp.1095, 2002.

Zhang, Y., Yao, T. D., and Pu, J. C.: The characteristics of ablation on continental-type glaciers in China, Journal of Glaciology and Geocryology, 18(2), 147-154, 1996 (in Chinese).

Zhang, Y., Wang, C., and Bai, W., et al.: Alpine wetland in the Lhasa River Basin, China, Journal of Geographical Sciences, 20(3): 375-388, 2010 (in Chinese).

Zhang, Z. X., Chang, J., and Xu, C. Y., et al.: The response of lake area and vegetation cover variations to climate change over the Qinghai-Tibetan Plateau during the past 30 years, Science of the Total Environment, 635, 443-451, 2018.

Zhou, Y. W., Guo, D. X., Qiu, G. Q., Cheng, G. D., and Li, S. D.: Permafrost in China, Science Press, Beijing, pp. 63-70, 2000 (In Chinese).

606 Zou, D., Zhao, L., Sheng, Y., and Chen, J., et al.: A new map of permafrost
607 distribution on the Tibetan Plateau, The Cryosphere, 11, 2527-2542,
608 doi:10.5194/tc-11-2527-2017, 2017.
609

610

Table 1. Mann-Kendall trend test with trend-free pre-whitening of seasonal and annual mean air temperature (°C), precipitation (mm), streamflow (mm), baseflow (mm) and quick flow (mm) from 1979 to 2013.

	Air temperature		Precipitation		Streamflow		Baseflow		Quick flow	
	Z_C	β (°C/a)	Z_C	β (mm/a)	Z_C	β (mm/a)	Z_C	β (mm/a)	Z_C	β (mm/a)
Spring	2.73**	0.026	0.90	0.290	3.05**	0.206	2.99**	0.147	0.98	0.042
Summer	2.63**	0.013	1.30	2.139	0.92	0.549	1.27	0.429	0.50	0.128
Autumn	2.65**	0.024	-0.68	-0.395	2.46*	0.546	2.96**	0.476	0.80	0.074
Winter	3.49**	0.051	-0.46	-0.014	3.08**	0.204	2.13*	0.145	1.39	0.016
Annual	4.48**	0.028	1.28	2.541	2.07*	1.230	2.70**	1.095	0.77	0.327

Comment: the symbols of Z_C and β mean the standardized test statistic and the trend magnitude, respectively; positive values of Z_C and β indicate the upward trend, whereas negative values indicate the downward trend in the tested time series; the symbols of asterisks *and ** mean statistically significant at the levels of 5% and 1%, respectively.

Table 2. Gray relational grades between the streamflow/baseflow and climate factors (precipitation and air temperature) in the Yangbajain Catchment at both annual and seasonal scales. Bold text shows the higher gray relational grade in each season.

	G_{oi} with the streamflow		G_{oi} with the baseflow	
	Precipitation	Air temperature	Precipitation	Air temperature
Spring	0.690	**0.778**	0.713	**0.789**
Summer	0.689	**0.784**	0.680	**0.776**
Autumn	0.653	**0.667**	0.648	**0.680**
Winter	0.742	**0.886**	0.748	**0.895**
Annual	0.675	**0.727**	0.665	**0.729**

611 Comment: G_{oi} is the gray relational grade between the streamflow/baseflow and climate factors. The importance of each influence factor can be determined by the
612 order of the gray relational grade values. The influence factor with the largest G_{oi} is regarded as the main stress factor for the objective variable.

613 Table 3. The coverage of glaciers and frozen ground in four catchments of the Lhasa River Basin

Stations	Area (km^2)	Glaciers(1960)		Glaciers(2009)		Permafrost (1996)		Permafrost (2017)		Seasonally frozen ground (1996)		Seasonally frozen ground (2017)	
		Area (km^2)	Coverage (%)	Area (km^2)	Coverage (%)	Area (km^2)	Coverage (%)	Area (km^2)	Coverage (%)	Area (km^2)	Coverage (%)	Area (km^2)	Coverage (%)
Lhasa	26233	349.26	1.3	347.14	1.3	10535	40.2	9783	37.3	15698	59.8	16450	62.7
Pangdo	16425	345.24	2.1	339.90	2.1	8666	52.7	8242	50.2	7762	47.3	8184	49.8
Tangga	20152	348.12	1.7	342.27	1.7	10081	50.0	9432	46.8	10071	50.0	10720	53.2
Yangbajain	2645	316.31	12.0	278.26	10.5	1352	51.1	946	35.8	1293	48.9	1699	64.2

614

615 Table 4. Mann-Kendall trend test with trend-free pre-whitening of annual mean air temperature (°C), precipitation (mm) and streamflow (mm) in
616 four catchments of the Lhasa River Basin

	Air temperature		Precipitation		Streamflow	
	Z_C	β (°C/a)	Z_C	β (mm/a)	Z_C	β (mm/a)
Lhasa	6.07**	0.028	1.16	1.581	1.09	1.420
Pangdo	6.19**	0.026	0.89	1.435	0.30	0.223
Tangga	7.35**	0.021	1.48	2.005	-0.62	-0.531
Yangbajain	4.48**	0.028	1.28	2.541	2.07*	1.230

617

Figure captions

Figure 1. (a) The location, (b) elevation distribution, and (c) glacier and frozen ground distribution (Zou et al., 2017) in the Yangbajain Catchment of the Lhasa River Basin in the TP.

Figure 2. Seasonal variation of streamflow (*R*), mean air temperature (*T*), and precipitation (*P*) in the Yangbajain Catchment.

Figure 3. Diagram depicting surface flow and groundwater flow due to glacier melt and permafrost thawing under (a) past climate and (b) warmer climate.

Figure 4. Variations of annual (a) streamflow and (b) baseflow from 1979 to 2013.

Figure 5. Variations of annual (a) mean air temperature and (b) precipitation from 1979 to 2013.

Figure 6. Variations of seasonal streamflow and baseflow in (a) spring, (b) summer, (c) autumn, and (d) winter from 1979 to 2013.

Figure 7. Variations of seasonal mean air temperature in (a) spring, (b) summer, (c) autumn, and (d) winter from 1979 to 2013.

Figure 8. Recession data points of $-dy/dt$ versus y and fitted recession curves by decades in log-log space. The black point line, dotted line, and solid line represent recession curves in the 1980s, 1990s, and 2000s, respectively.

Figure 9. Variations of (a) the recession coefficient K and (b) groundwater storage S from 1979 to 2013.

Figure 10. Variations of annual NDVI from 1998 to 2013 in the catchment.

639 **Figure 11.** The total area and volume of glaciers in the Yangbajain Catchment in 1960

640 and 2009.

641

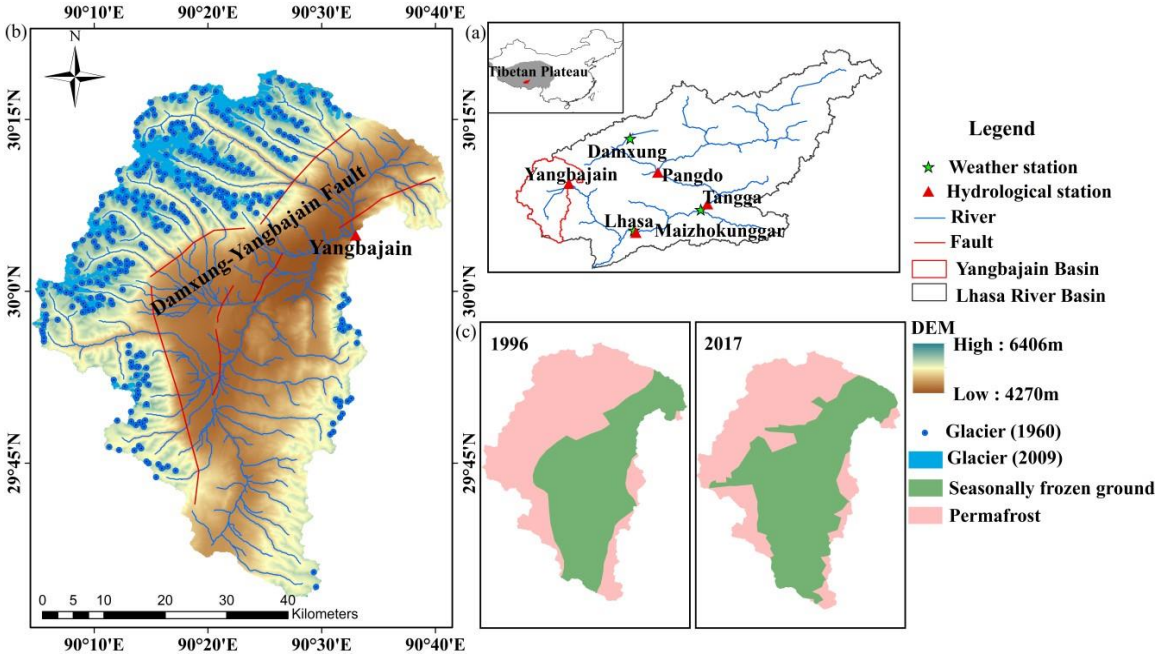

Figure 1. (a) The location, (b) elevation and glacier distribution for the twice Chinese Glacier Inventory, only the location of glacier snouts in 1960 were provided in the first Chinese Glacier Inventory, and the boundaries of glaciers were shown in the second Chinese Glacier Inventory, and (c) twice maps of frozen ground distribution (Li and Cheng, 1996; Zou et al., 2017) in the Yangbajain Catchment.

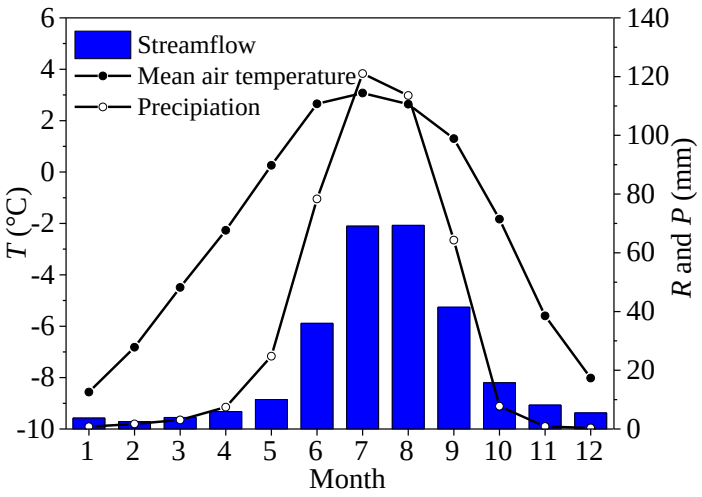

649

650 **Figure 2.** Seasonal variation of streamflow (*R*), mean air temperature (*T*), and

651 precipitation (*P*) in the Yangbajain Catchment.

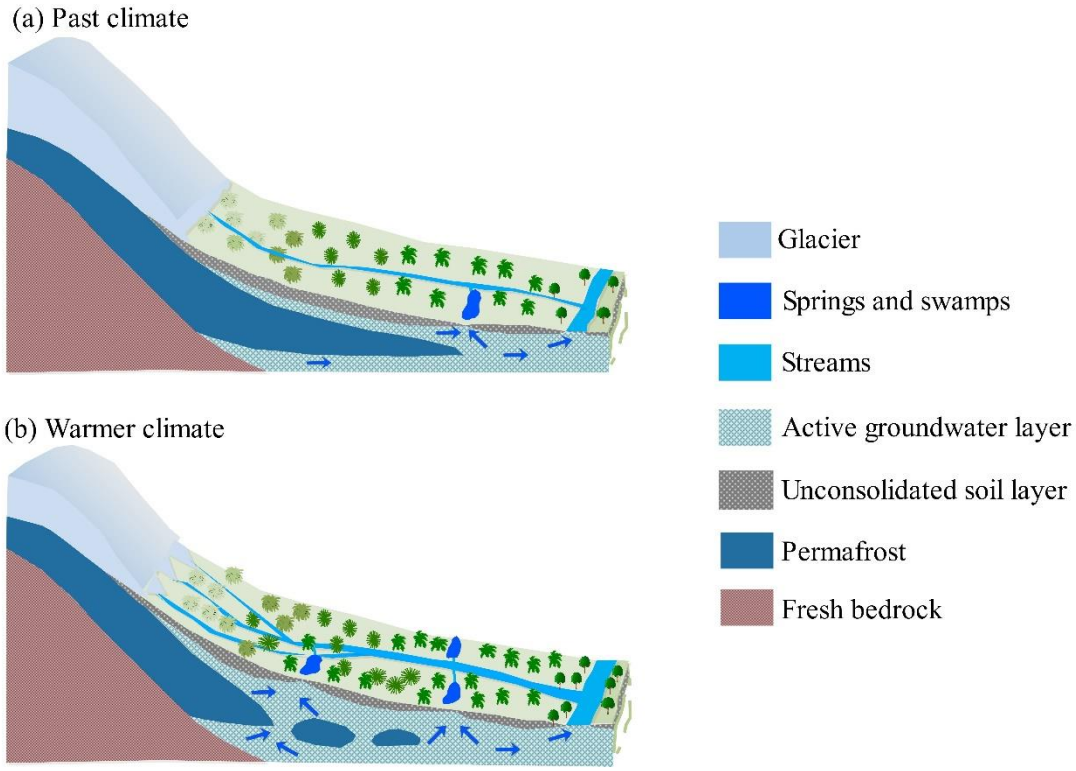

652

653 **Figure 3.** Diagram depicting surface flow and groundwater flow due to glacier melt

654 and permafrost thawing under (a) past climate and (b) warmer climate.

655

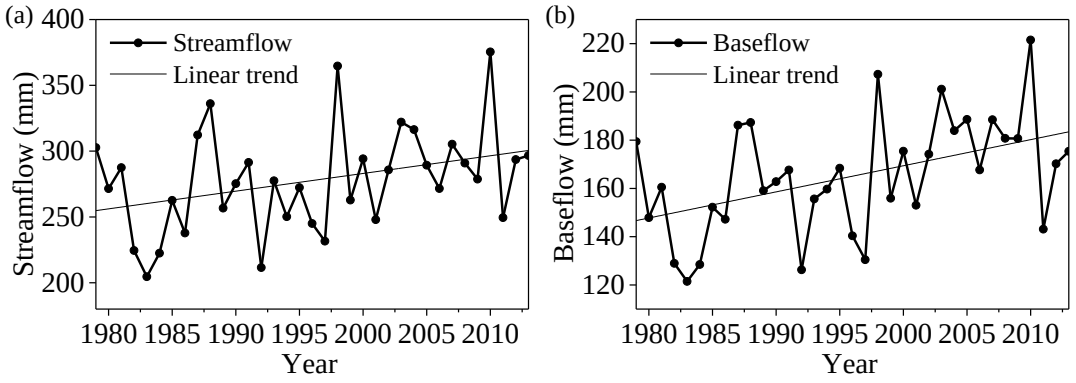

656

657 **Figure 4.** Variations of annual (a) streamflow and (b) baseflow from 1979 to 2013.

658

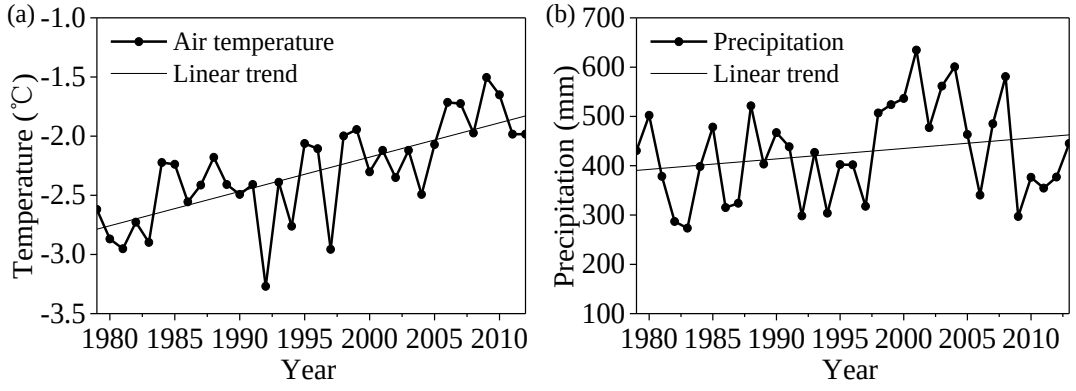

659

660 **Figure 5.** Variations of annual (a) mean air temperature and (b) precipitation from

661 1979 to 2013.

662

663

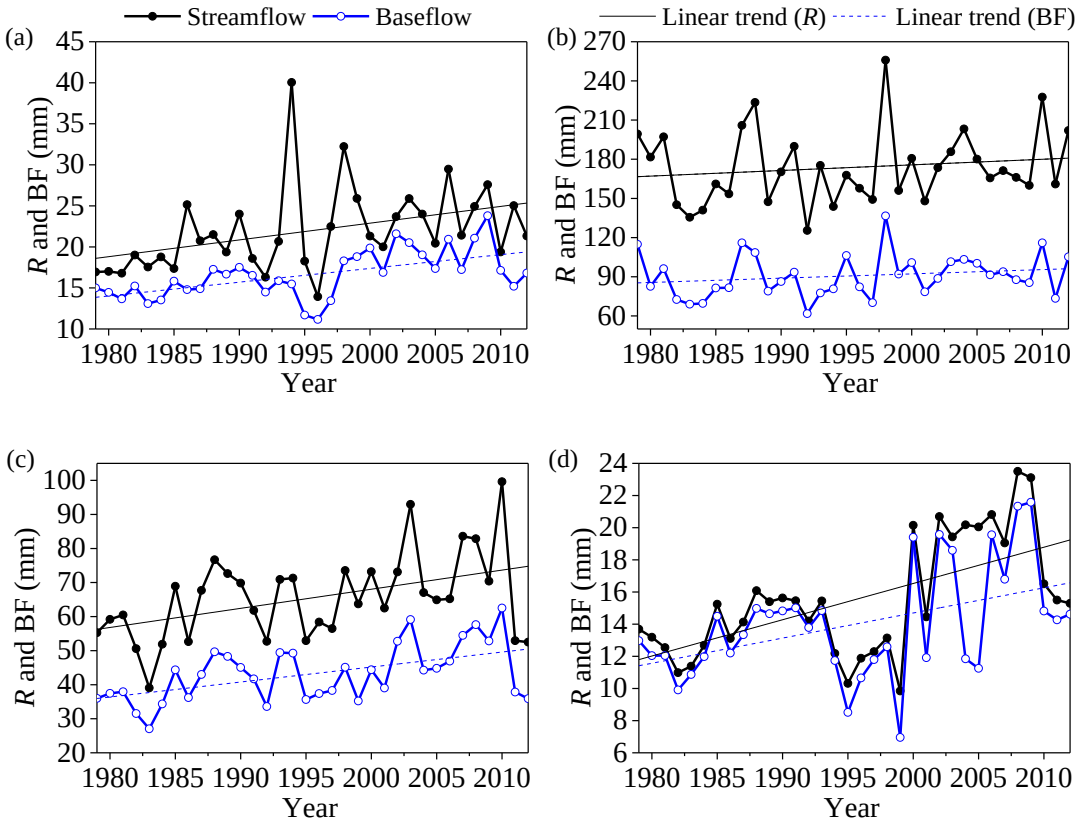

664

665 **Figure 6.** Variations of seasonal streamflow and baseflow in (a) spring, (b) summer,

666 (c) autumn, and (d) winter from 1979 to 2013.

667

668

669

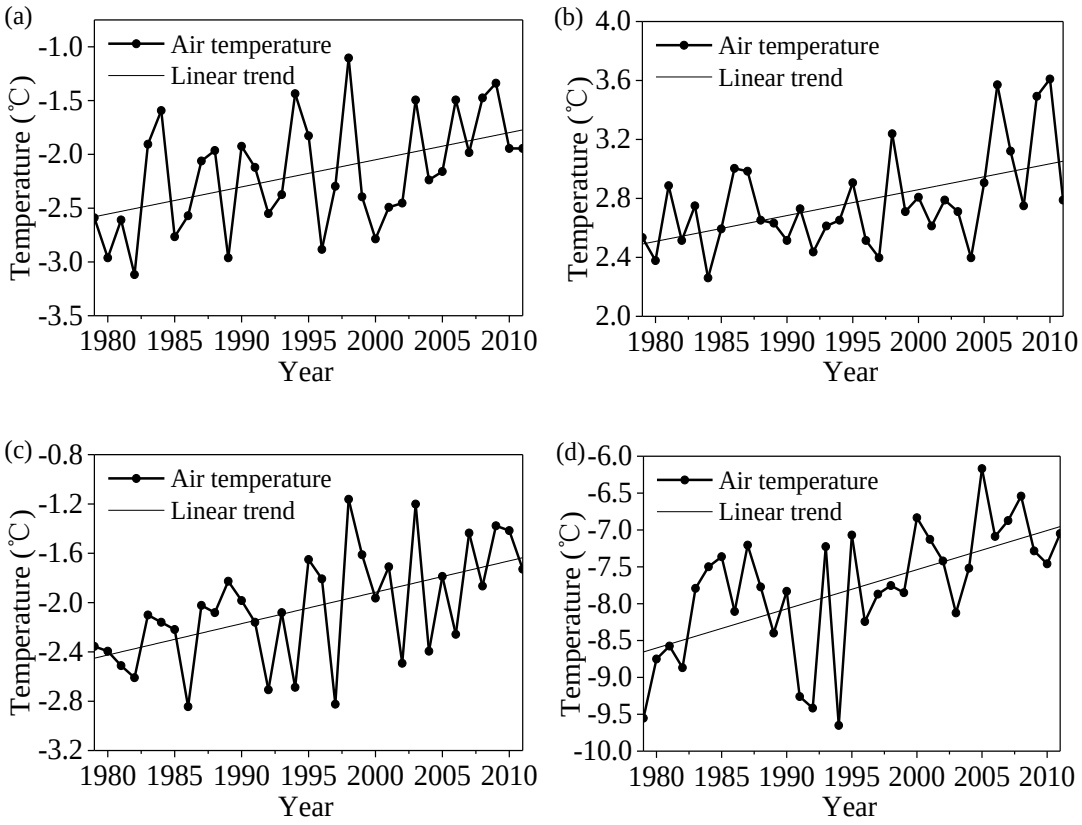

670

671 **Figure 7.** Variations of seasonal mean air temperature in (a) spring, (b) summer, (c)

672 autumn, and (d) winter from 1979 to 2013.

673

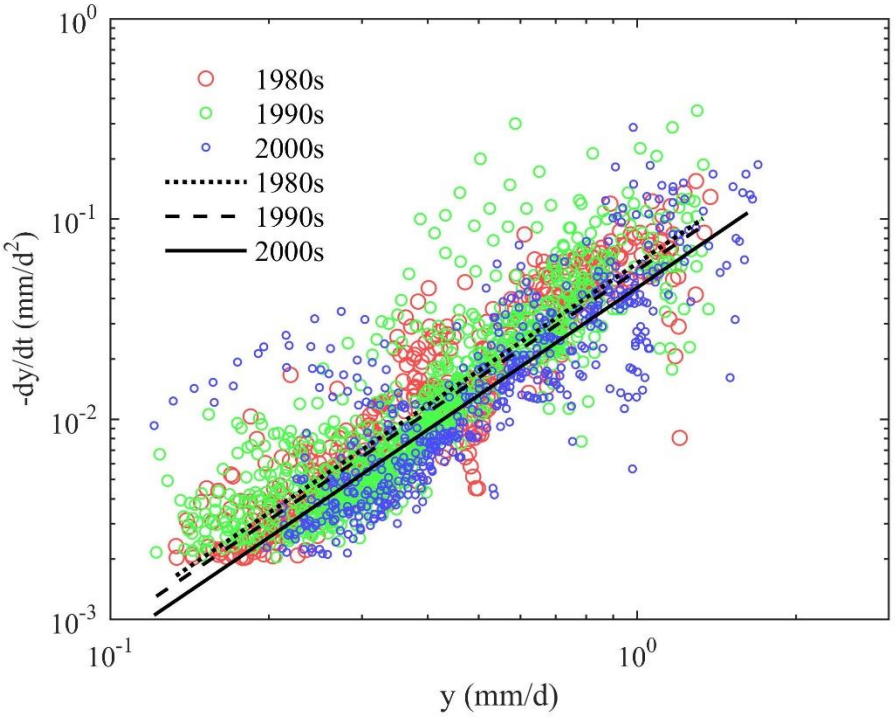

Figure 8. Recession data points of *-dy/dt* versus *y* and fitted recession curves by decades in log-log space. The black point line, dotted line, and solid line represent recession curves in the 1980s, 1990s, and 2000s, respectively.

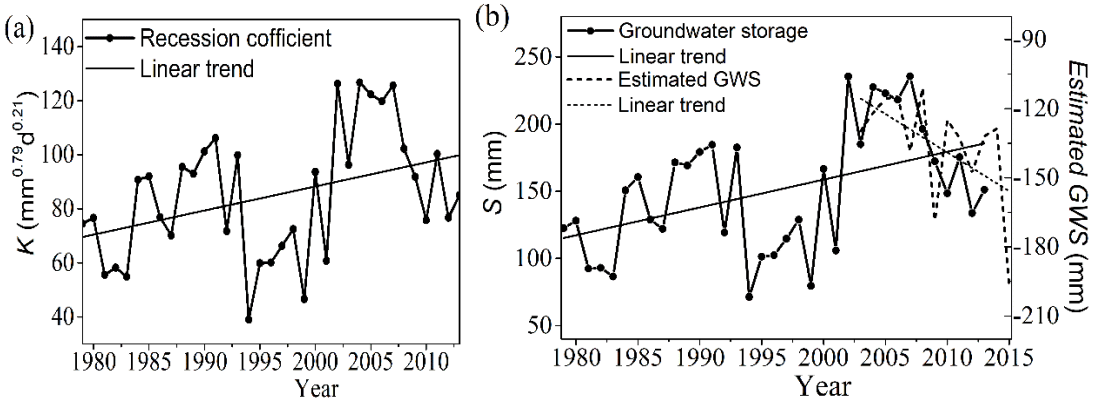

Figure 9. Variations of (a) the recession coefficient *K* and (b) the estimated groundwater storage *S* from 1979 to 2013 and the estimated groundwater storage change from 2003 to 2015 by GRACE data.

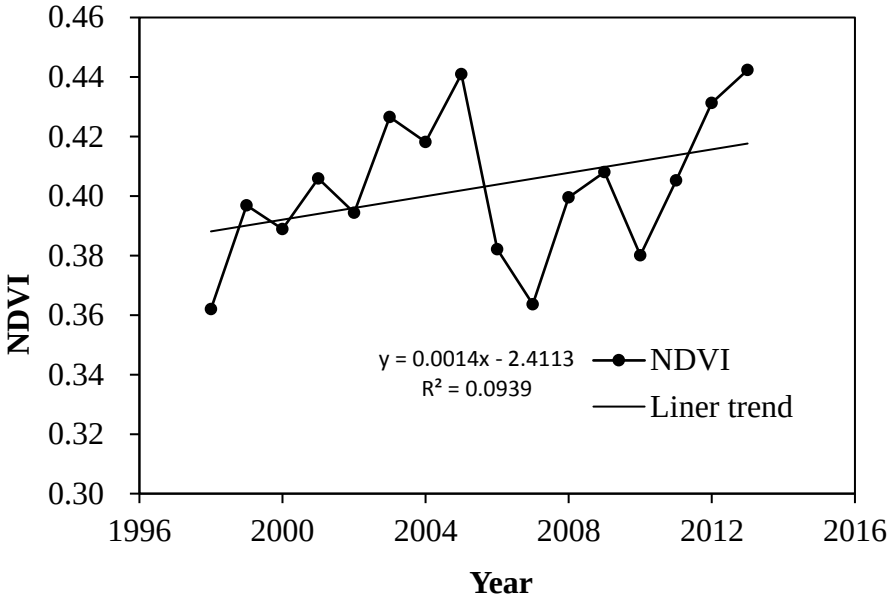

684

685 **Figure 10.** Variations of annual NDVI from 1998 to 2013 in the catchment.

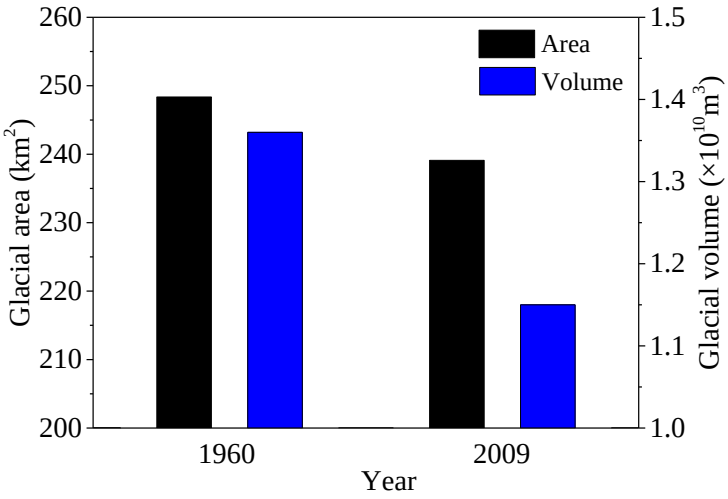

686

687 **Figure 11.** The total area and volume of glaciers in the Yangbajain Catchment in 1960

688 and 2009.

689